

## THE STRUCTURE OF BRIGHTEST CLUSTER MEMBERS. III. cD ENVELOPES

JAMES M. SCHOMBERT<sup>1, 2</sup>

Palomar Observatory, California Institute of Technology; and Yale University Observatory

Received 1987 July 6; accepted 1987 November 9

### ABSTRACT

Single-band photographic and CCD surface photometry is used to determine luminosity and structural properties of the extended, faint envelopes around 27 cD galaxies. The distribution of envelope light follows a similar slope ( $I \propto r^{-1.6}$ ) as other cluster luminous material (i.e., galaxies). Several correlations between envelope luminosity and cluster properties (richness, cluster X-ray luminosity, Bautz-Morgan type, and Rood-Sastry type) substantiate arguments for the dynamical formation of envelopes. A correlation between underlying galaxy luminosity and envelope luminosity implies a parallel but separate process between the growth of the first-ranked elliptical by mergers and cD envelope formation. Strong color gradients, in particular the blue disk colors as predicted by other studies, were not found upon examination of multicolor profiles for three cD envelopes.

*Subject headings:* galaxies: clustering — galaxies: photometry — galaxies: structure

### I. INTRODUCTION

Galaxies classified as cD occupy a special place in the scheme of extragalactic structure by being intermediate in scale between normal galaxies and cluster-sized entities and may be important for tracing the behavior of cluster dynamics (see review by Tonry 1987). Their faint extended appearance and tremendous size were first discovered from visual inspection of photographic plates by Matthews, Morgan, and Schmidt (1964); however, the outstanding nature of extended envelopes (radii in excess of 1.5 Mpc in some cases) was not revealed until the faint surface photometry of Oemler (1976). It soon became apparent that the existence of true cD envelopes, rather than merely shallow profiles, was a subject only suitable for study using deep surface photometry (Malumuth 1983). It has also been found that many visually classified cD galaxies exist without extended envelopes, as well as a few non-first-ranked galaxies with cD envelopes (e.g., NGC 6034 in Hercules, see Schombert 1986, hereafter Paper I, and Schombert 1987, hereafter Paper II). This paper will consider only those distinct envelopes which break from the surface brightness profiles of D and cD galaxies; the diffuse outer regions found around many brightest cluster galaxies will not be discussed.

The enormous size of extended envelopes implies that the outer regions must be strongly influenced by the cluster potential and that they reflect the dynamics of cluster orbits rather than the kinematics of the underlying galaxy (see also Dressler 1979). Information about the cD envelope yields knowledge of the cluster potential near the center of rich clusters. Therefore, this paper will investigate the possible correlations between optical and nonoptical cluster dynamical state indicators and the properties of pure cD envelopes in search of clues to their formation and evolution.

There have been many attempts to explain the origin of cD

envelopes. The four leading hypotheses are stripping theory (Gallagher and Ostriker 1972; Richstone 1976; Malumuth and Richstone 1984), cooling flows (Fabian and Nulsen 1977; Cowie and Binney 1977; Fabian, Nulsen, and Canizares 1984), mergers (Villumsen 1982; Duncan, Farouki, and Shapiro 1983), and the primordial origin theory (Merritt 1984). Each has its own predictions, although stripping and primordial origin operate with similar processes. Stripping theory proposes that the extra luminosity component of cD galaxies has its origin in stars removed from cluster members through tidal interactions and then deposited on the central galaxy. Merritt (1984) argues that there is no need to impose a special process for creating extended envelopes and hypothesizes that all galaxies had large halos early in the life of a cluster. These halos were then removed by the mean cluster tidal field during the initial collapse and returned to the cluster potential, except for the central member (i.e., the cD galaxy). Its envelope remains unaffected because of its special position with respect to the cluster potential and, thus, inherits the remnants of other halos. The main difference between stripping and primordial origin is that stripping begins after cluster collapse and is ongoing as the cluster evolves. Primordial origin assumes that the strong tidal events occur before collapse and that there is little activity after cluster virialization.

Two other formation methods are cooling flows and mergers. Cooling flow theory introduces the idea that radiative cooling of hot X-ray gas decreases its pressure and, then, this denser gas settles toward the center of the potential. If there is a central member at this location, this gas can collect until sufficient densities are reached to begin star formation (Fabian, Nulsen, and Canizares 1984). Mergers are usually invoked to increase the interior luminosity of first-ranked ellipticals; however, under special conditions it may be possible to increase the energy of the outer regions so that they distend into an extended envelope.

There have been several studies in the last 15 years which link the properties of clusters to the luminosity of cD galaxies (Sandage and Hardy 1973; Malumuth and Kirshner 1981; Schneider, Gunn, and Hoessel 1983). However, most of these works have treated the cD galaxy as a whole unit without attempting to separate the cD envelope from the parent BCM

<sup>1</sup> Visiting Astronomer, Cerro Tololo Inter-American Observatory, under contract with the National Science Foundation

<sup>2</sup> Visiting Astronomer, Kitt Peak National Observatory, operated by the Association of Universities for Research in Astronomy, Inc., under contract with the National Science Foundation. Observations made with the Burrell Schmidt of the Warner and Swasey Observatories, Case Western Reserve University.

(brightest cluster member, first-ranked elliptical). The closest procedure to separation was the work of Malumuth and Kirshner (1981), who measured an excess luminosity for each cD galaxy from what was expected based on its central velocity dispersion and the Faber-Jackson relation. However, the parent galaxy owes most of its luminosity growth to merges (see Paper II), whereas there are several possible origins for extended envelopes.

The purpose of this paper is to use the deep surface photometry from Papers I and II to determine the luminosity, colors, and structural properties for a sample of cD envelopes independent of the underlying BCM. These values can then be compared to the global properties of clusters in order to test the effect of environment on cD envelopes. The observations and data reduction are presented in § II along with a list of objects. Properties of envelopes are discussed in §§ IIIa and IIIb. A simple two-component model for galaxy and envelope light is constructed and compared to observations in § IIIc. The comparison to cluster parameters is presented in § III d.

## II. OBSERVATIONS AND REDUCTION

As discussed in Paper II, the term cD galaxy will be used only for those bright ellipticals which, when examined with deep surface photometry, display the characteristic extended envelope breaking from the main profile (see examples in Paper II). This envelope has little to do with the visual estimate of "cD-ness", a term which is more closely related to the slope of the galaxy profile than an indicator of true envelopes (Malumuth 1983). Table 1 lists those galaxies with clearly

defined extended envelopes from Paper II and that meet the observational constraints outlined below.

Photographic material is often necessary to measure the outer edges of extended envelopes in nearby clusters. The usual choice is wide field plate material from Schmidt telescopes. Schmidt plates have ideal scales for measuring the envelopes, although they sacrifice information on the cores of the cD galaxy. Plate material also provides a large number of pixels per isophote, which is a requirement for sufficient sky contrast to reach the  $28V$  mag arcsec $^{-2}$  level representative of many cD envelopes. CCD systems usually have limited field sizes do not encompass the full extent of cD envelopes with a reasonable amount of empty sky. When CCD frames are used in this study, the existence of a cD envelope was first noted on the photographic material and then reobserved with the Palomar 1.5 m RCA CCD system and reimaging optics. For the more distant clusters, CCD frames were sufficient. Reduction methods for photographic material are outlined in Paper I; CCD methods are outlined in Paper II.

In addition to the objects from Papers I and II, a new cD galaxy, NGC 4874 in Coma, was added using the surface photometry from Baum, Thomsen, and Morgan (1986). From the definition of a cD galaxy in Paper II, and comparison to standard elliptical templates, it can be stated with a high degree of confidence that NGC 4874 is a true cD galaxy. The Coma cluster now has the distinction of being the first system to contain two cD galaxies (NGC 4874 and NGC 4839; Oemler 1976). NGC 4874 is more dominant in size, luminosity, and location than NGC 4839, and thus is probably the center of the

TABLE 1  
CD ENVELOPES

Cluster (1)	Galaxy (2)	RS Type <sup>a</sup> (3)	BM Type <sup>b</sup> (4)	log $L_{gal}$ (5)	log $L_{env}$ (6)	log $r_e$ (7)	$\mu_e$ (8)	$\beta$ (9)
A150	UGC 716	cD	I-II	10.92	10.84	1.59	24.96	-1.63
A151	G1	cDs	..	11.05	11.08	1.70	24.93	-1.71
A358	G1	C	..	10.96	11.06	1.60	24.84	-1.54
A400	G1	Ic	II-III	10.63	10.47	1.85	26.31	-1.54
Perseus	NGC 1275	L	II-III	11.10	10.22	2.45	28.66	-1.41
A779	NGC 2832	cDs	I-II	10.92	9.50	0.95	22.04	-2.35
A1413	G1	cD	I	11.53	11.85	3.03	29.81	-1.34
Coma	NGC 4874	..	..	11.63	11.03	2.01	25.34	-1.52
	NGC 4839 <sup>c</sup>	..	..	10.86	10.18	2.83	30.73	-1.24
A1767	G1	cD	II	11.11	10.95	2.03	26.02	-1.28
A1795	Zw 162010	cD	I	11.00	11.28	1.38	23.47	-1.54
A1809	G1	cD	II	11.16	10.93	1.83	25.61	-1.68
A1904	G1	C	II-III	11.13	10.52	1.59	24.53	-1.51
A1913	Zw 104027	Ic	III	10.69	10.48	1.53	25.29	-1.72
A2142	G1	B	II	11.45	11.14	1.91	25.13	-1.39
A2147	UGC 10143	F	III	11.10	11.16	2.23	26.99	-1.33
Hercules	NGC 6034 <sup>c</sup>	..	..	10.96	10.87	2.37	28.34	-1.35
A2162	NGC 6086	Is	II-III	10.85	10.99	1.53	24.39	-1.64
A2199	NGC 6166	cD	I	11.21	10.74	2.00	26.24	-1.82
A2366	G1	F	I-II	11.02	10.52	1.51	24.68	-2.03
A2420	G1	cD	I	11.16	10.68	1.89	25.72	-1.49
A2572	NGC 7597	F	III	10.84	10.57	1.37	24.03	-1.73
A2589	NGC 7647	cD	I	10.92	10.82	1.76	25.34	-1.69
A2634	NGC 7720	cD	II	10.99	10.26	1.61	25.21	-2.10
A2670	G1	cD	I-II	11.25	11.31	2.52	28.31	-1.57
SC1325-31	G1	cD <sup>d</sup>	I <sup>d</sup>	11.27	12.04	3.20	29.42	-1.18
SC1331-31	G1	cD <sup>d</sup>	I-II <sup>d</sup>	11.27	10.97	1.59	24.02	-2.20

<sup>a</sup> Rood-Sastry types from Struble and Rood 1987b.

<sup>b</sup> Bautz-Morgan types from Leir and van den Bergh 1977.

<sup>c</sup> Non-first-ranked cluster members.

<sup>d</sup> Estimated off of UK/SERC Southern Sky Survey.

main cluster potential. This should have important ramifications to Coma dynamical studies (see Fitchett and Webster 1987).

In order to obtain luminosity values for cD envelopes which were free of the underlying galaxy's contribution, it was necessary to subtract the effects of the parent system. The best method, as discussed in Papers I and II, was to remove a template elliptical profile that fit the inner regions of the cD galaxy (see example in Fig. 1). These templates were drawn from a sample of bright ellipticals in clusters and the field (excluding first ranked members). Although it is not clear what effect the cD envelope has on the outer structure of ellipticals, this was the most straight forward method of removing underlying galaxy light. Other methods of galaxy subtraction (e.g., removing best-fit  $r^{1/4}$  components) yielded similar results. Table 1 summarizes the data for the 27 cD galaxies of this study. The cluster and parent galaxy name are listed in columns (1) and (2). The Rood-Sastry and Bautz-Morgan types (Struble and Rood 1987*b*) are listed in columns (3) and (4). The luminosities for the underlying galaxy ( $L_{\text{gal}}$ ) and the cD envelope ( $L_{\text{env}}$ ) are listed in columns (5) and (6) in units of solar luminosity assuming an absolute magnitude for the Sun of  $M_V = 4.77$  and a  $H_0 = 100 \text{ km s}^{-1} \text{ Mpc}^{-1}$ . Fits of the cD envelope to the  $r^{1/4}$  law (discussed in § IIIc) are listed in columns (7) and (8). The power-law slope,  $\beta$ , of the cD envelope is listed in column (9).

Errors resulting from the subtraction process were closely related to errors in the faint light levels between the envelopes and measured sky values. Comparisons between different templates and multiple profiles of the same cD galaxy gave an average error of  $\pm 0.10$  (log  $L$ ) for the envelope luminosities in Table 1. The largest error was associated with those envelopes with the shallowest slopes, where small deviations in the photometry produced large variations in calculated luminosity. A lower bound of  $\log L_{\text{env}} = 9.0$  (e.g., see the profile for A779 in Paper I) was set by the impossibility of detecting such faint

envelopes superposed on the dominant light of the galaxy. An upper bound was limited only by the field size and the ability to determine the sky level to a given accuracy.

Color profiles were produced for a selected subsample of cD and D type galaxies (Schombert 1988). Three objects from that sample with cD envelopes (NGC 6034, A1767-G1, and A1413-G1) are discussed in § IIIb. The objects were selected by requiring that the envelope fit on a single frame with room for sky measurements at both ends. Reduction of multicolor surface photometry from the Palomar 1.5 m CCD system is outlined in Schombert and Wallin (1987). Preliminary reduction and CLEANing used the image processing package ARCHANGEL on the Caltech Astronomy Department's VAX 11/780. Final reduction used an updated version of GASP (Galaxy Surface Photometry) developed by M. Cawson (Steward Observatory), with several modifications by G. Bothun (University of Michigan) and the author. Color profiles were produced by direct subtraction (in mag arcsec $^{-2}$ ) between the surface brightness profiles in the various bandpasses. Conversion to kiloparsecs was made using the redshifts of Struble and Rood (1987*a*), corrected for a Virgo infall of  $300 \text{ km s}^{-1}$ . A  $H_0$  of  $100 \text{ km s}^{-1} \text{ Mpc}^{-1}$  and a  $q_0$  of 0 have been assumed.

### III. DISCUSSION

#### a) Envelope Luminosities

Although extended envelopes in cD galaxies are faint in average surface brightness, they are large in area. This yields total integrated luminosities which are comparable to the luminosity of the underlying galaxy. Some of the envelopes from Paper I (e.g., A1413-G1 in Fig. 1) had no obvious cutoffs. In these cases, a pragmatic cutoff was assumed at the  $30V$  mag arcsec $^{-2}$  level. Those profiles which do have cutoffs may have errors in their estimated sky level, thereby producing a sharp drop in the outer envelopes. Hence, the issue of how the edges

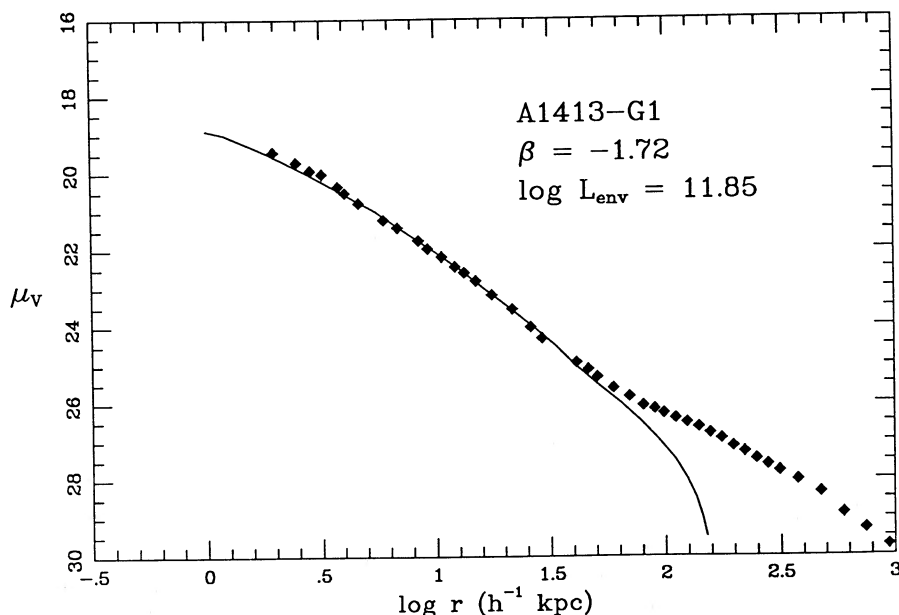


FIG. 1.—Surface brightness profile for the cD galaxy in A1413 (Oemler 1976) along with best-fit template from Paper II. Envelope luminosities in Table 1 are determined by direct subtraction of the template from the data, then summation of the remaining luminosity. This system contains one of the brighter envelopes in the sample.

of cD envelopes merge into the background cluster light and whether this change is abrupt or smooth is not resolved (see also Porter 1987).

Since there is little surface photometry of cD envelopes in the literature, external checks of envelope luminosity are not possible. However, it was shown in Paper I that the major contributor to error at low light levels is from errors in the estimated sky. Other contributors to error are improper zero-point, incorrect redshift, galactic absorption, and contamination by stars or galaxies. To counter these effects, the reduction techniques were designed to minimize photometric errors. In order to test the effects of sky error on the envelope measurements, some simple numerical tests were constructed to reproduce the profiles for varying sky values by  $\pm 3 \sigma$  the background noise. The result was that cD envelope luminosities are only affected at the  $\pm 10\%$  level (mildly dependent on profile slope).

It can be noted from inspection of Table 1 that, to first order, the galaxy and envelope luminosities are comparable. If the  $M/L$  of cD envelopes is similar to giant ellipticals (i.e.,  $M/L = 5-10$ ; Malumuth and Kirshner 1985) then the mass in a cD envelope contributes only as much mass to the cluster as one bright elliptical in the core. On the other hand, if the  $M/L$  values of cD envelopes are similar to the  $M/L$  envelope values for the giant D galaxy in A2029 (i.e.,  $M/L = 275$ ; Dressler 1979), then they may cause significant dynamical friction effects. If this  $M/L$  value is constant, then cD envelopes would also contain up to 15 times the mass of a first-ranked elliptical or  $10^{13} M_{\odot}$ .

A comparison of galaxy and envelope luminosities,  $\log L_{\text{env}}$  versus  $\log L_{\text{gal}}$  in solar units, is shown in Figure 2.  $L_{\text{env}}$  is weakly correlated with  $L_{\text{gal}}$  (a standard least-square correlation coefficient of  $R = 0.6$ ), suggesting that cD envelopes share a common origin with the underlying galaxy (i.e., mergers; see Paper II). Several numerical studies (Villumsen 1982; Duncan, Farouki, and Shapiro 1983) have attempted to produce cD

envelopes with mergers. The hypothesis is that mergers transfer significant energies to distend the outer regions of the remnant into cluster-sized envelopes. However, these simulations were only able to achieve envelopes whose luminosities were 10% the luminosity of the underlying galaxy. A majority of the stars were still contained in the main body of the parent galaxy and not in distended envelopes. In particular, the remnants did not span the Mpc scale seen in this data sample, and the luminosities were an order of magnitude below the average envelopes luminosities listed in Table 1.

The basic reason for the failure of mergers to form cD envelopes comes from energy considerations. The standard criterion for a merger is that the orbital velocity (i.e., orbital energy) be less than or similar to the velocity dispersion of the BCM (i.e., internal energy; White 1982). This value of  $300 \text{ km s}^{-1}$  for most BCMs is much less than the velocity dispersion required of a Mpc-sized envelope. Since the luminosity of cD envelopes is often greater than the luminosity of the underlying galaxy, the possibility of a majority of the mass being heated to envelope scales by mergers or later tidal collisions is extremely unlikely. Thus, *mergers are insufficient as a source of cD envelope luminosity and scale*, but the correlation in Figure 2 is suggestive of a parallel process between the dynamical growth of a BCM and cD envelopes.

#### b) Envelope Colors

Stripping theory would propose that cD envelopes are predominately blue because low luminosity and disk systems are more numerous and easier to strip than giant ellipticals (White 1982). Strom and Strom (1977) discovered evidence of this process in several nearby clusters by detecting a difference in the mean structure of galaxies in the cores versus galaxies with orbits in the outer regions. Furthermore, they also determined that galaxies with strong blue color gradients are less common centrally than in the outer cluster regions. This is interpreted as the blue halos having stripped from low-luminosity objects,

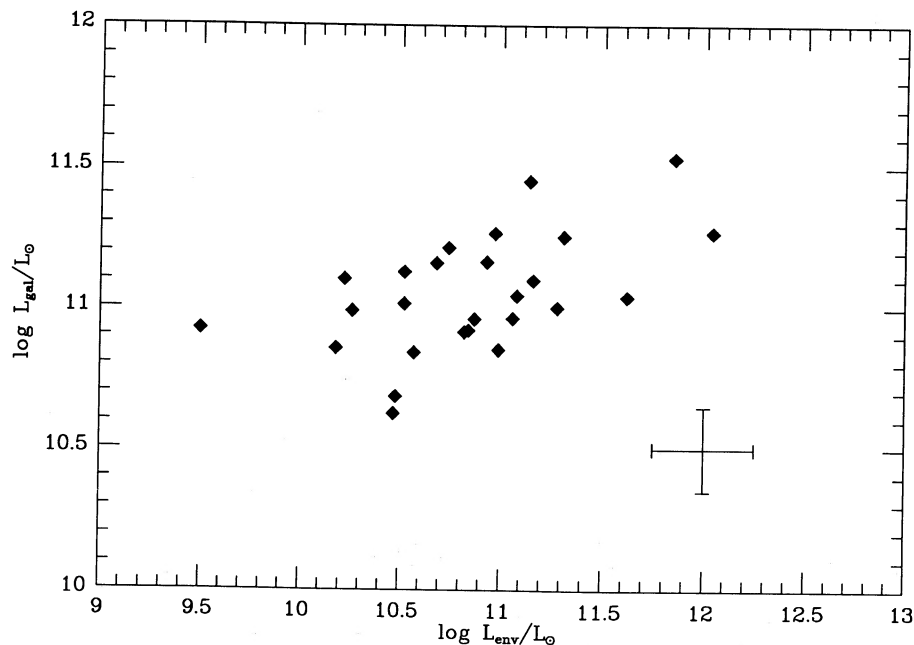


FIG. 2.—Luminosity of underlying galaxy,  $L_{\text{gal}}$ , vs. the luminosity of the cD envelope,  $L_{\text{env}}$ , in solar units. The weak correlation suggests a parallel process between cD envelope formation and the growth of the parent elliptical. Typical error bars are indicated.

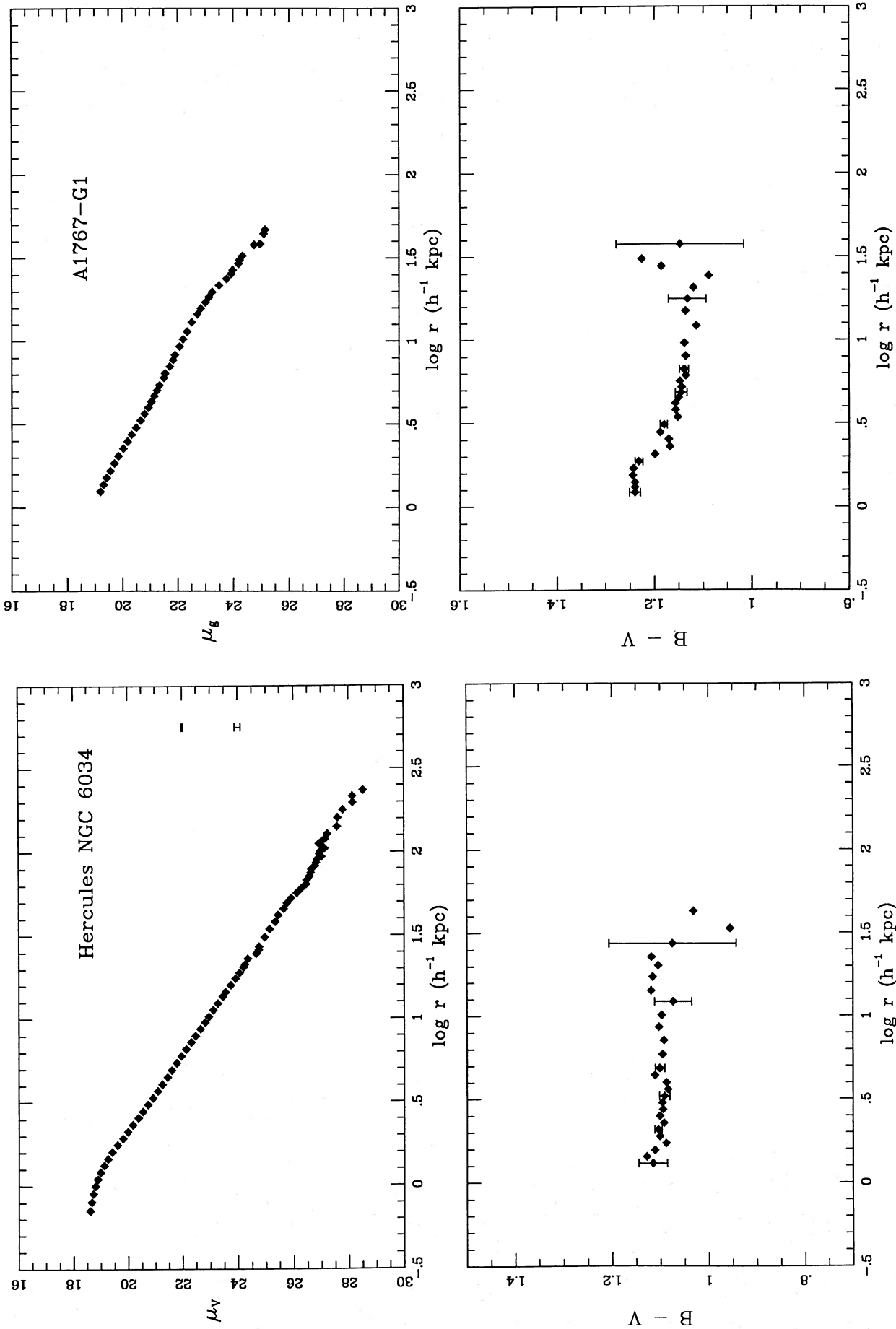


FIG. 3

(a) Surface brightness and  $B - V$  color profile for NGC 6034, a cD galaxy in Hercules. No evidence for blue envelope colors or any color gradient is found down to the  $25.5V$  mag arcsec $^{-2}$  level. (b) Surface brightness and  $B - V$  color profile for cD galaxy in A1767. (c) Surface brightness and  $B - V$  color profile for cD galaxy in A1413. Color data does not extend deep into the cD envelope, but no break or sharp gradient in color is detected at the edge of the envelope.

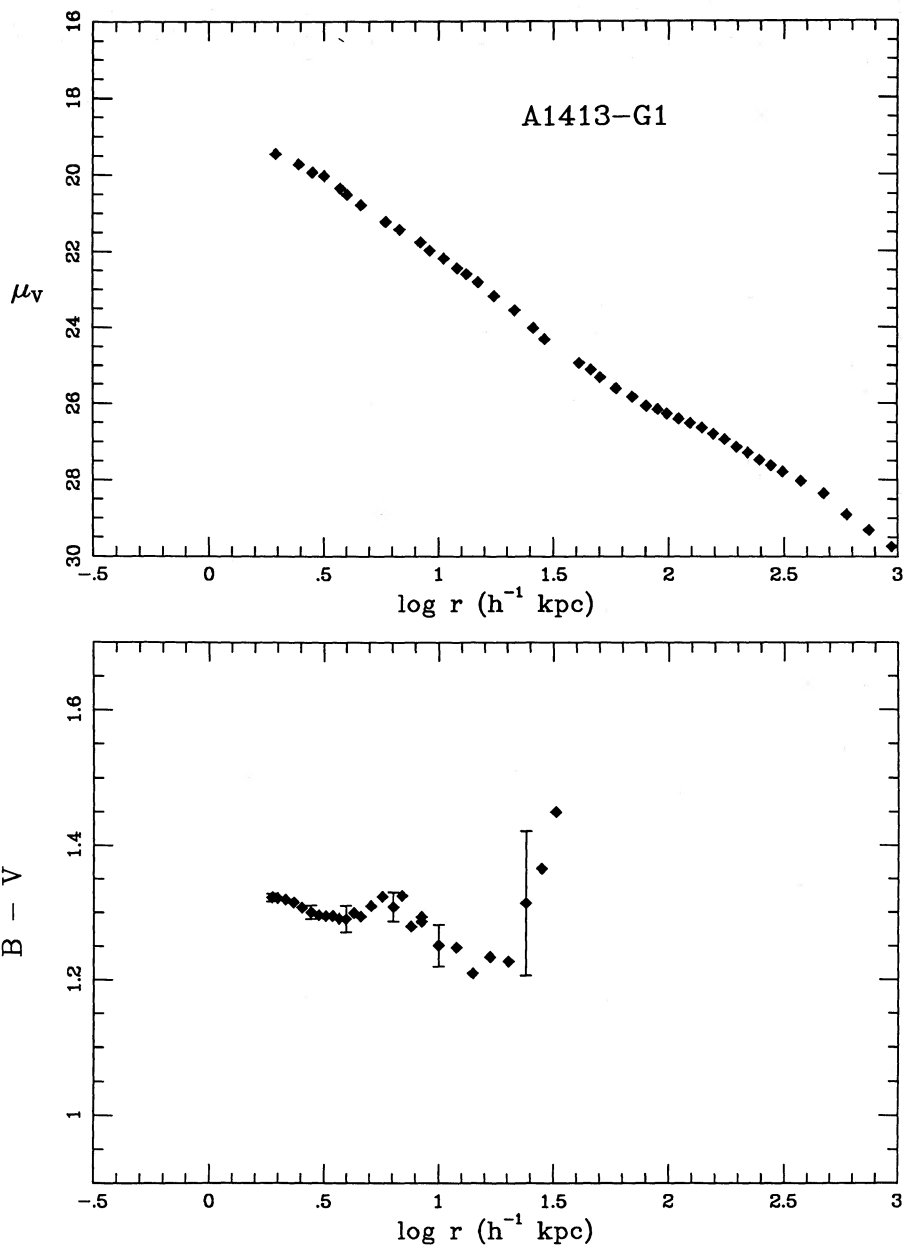


FIG. 3c

and this has reinforced the prediction that cD envelopes will appear bluer than normal giant elliptical colors.

Actual observations of the colors of cD galaxies are usually limited to aperture studies (Lugger 1984, and references therein) which indicated that cD galaxies are normal in color compared to other bright ellipticals. A more informative approach is that of Valentijn (1983) who obtained multicolor surface photometry (Johnson  $B$  and  $V$  bands). His data showed the existence of blue cD envelopes with multicolor profiles for five out of six cD galaxies in his sample displaying large color gradients [ $\Delta(B - V) = 0.4$ ], and outer envelope colors ranging from  $B - V$  of 0.5–0.7. This is the strongest evidence to date in support of the stripping hypothesis that accumulated matter is the content of cD envelopes. However, the study of V Zw 311 by Schneider and Gunn (1982), an example of a possible cD

galaxy in the process of formation, indicated that its envelope colors were red.

To further investigate this phenomenon,  $B - V$  profiles of three cD galaxies (NGC 6034, A1767-G1, and A1413-G1) were studied. Figure 3 displays the  $V$  surface brightness profile and  $B - V$  color profile for these objects. Note that the color information is deep into the envelope itself (with the exception of A1413-G1), and extends beyond the point where the parent galaxy light is expected to contribute 1% of the envelope light. Both color profiles for NGC 6034 and A1767-G1 extend into the inner edge of the cD envelope. The color of NGC 6034 is flat to the limit of the data. A1767-G1 displays a slight gradient, but the cD envelope has a mean color of  $B - V = 1.15$ . A1413-G1 displays a similar behavior with a  $B - V = 1.24$  at the point where the cD envelope dominates over the galaxy

light. No evidence of strong color gradients or blue envelope colors was found in any of the cD galaxies examined.

A double-blind experiment (Schombert and Bothun 1987) was undertaken to test the sensitivity of color gradient detection and whether strong gradients or blue colors could be hidden in the errors. The result was that a maximum gradient error of  $\Delta(B-V) = \pm 0.05$  is expected at cD envelope light levels; thus, any strong gradients would have been easily detected. Although the sample only consists of three objects, the lack of blue envelopes is in direct contradiction with the results of Valentijn (1983) and the expectation from the observations of Strom and Strom (1977). However, the lack of blue colors is in agreement with observations of V Zw 311 (Schneider and Gunn 1982). If stripping is the primary method of forming cD envelopes, then these colors imply that red galaxies rather than spirals are the source material. This is plausible since cD systems are only associated with high density regions (see § III d), and these regions are rich in early-type galaxies (Dressler 1980).

The lack of blue envelope colors also contradicts the expectation from cooling flows which produce a recent epoch of star formation. One possible solution was proposed by Fabian, Nulsen, and Canizares (1984). Their simulations which were able to form red, low-mass stars from cooling flows, and could produce similar colors to giant ellipticals. However, this star formation process should be confined to the cores of BCMs where the gas densities can develop to star formation thresholds, and seems unlikely as a method to form large extended envelopes.

### c) Envelope Structure

cD envelopes are relatively easy to distinguish from underlying galaxy surface brightness profiles due to the distinct break in the profile near the  $24V$  mag arcsec $^{-2}$  level. No contour information in outer regions of envelopes was attempted due to low signal-to-noise ratios of these regions. In

fact, the reduction software fixes the ellipse eccentricity and orientation at radii beyond which the  $S/N$  falls below a specified level to maintain a stable profile for determining faint envelopes. Nevertheless, there were no sharp changes in either eccentricity or position angle at the transition region from parent galaxy to cD envelope. No shells or bright features were seen in any of the profiles, possibly because these structures are short-lived due to tidal effects from other galaxies passing through the envelope (Lauer 1987). Alternatively, the relaxation time scales in the transition region are short (the average orbital time scale at these radii is  $10^8$  yr). Thus, the matching of the underlying galaxy contours with the envelope would be expected.

To determine typical scale lengths and characteristic surface brightness for cD envelopes, the underlying galaxy can be removed and remaining light fit to the  $r^{1/4}$  relation in the same manner as the bright ellipticals described in Paper II. Results of these fits are listed in Table 1 and displayed in Figure 4, a plot of effective radius,  $\log r_e$  in units of kpc, versus effective surface brightness,  $\mu_e$  in units of  $V$  mag arcsec $^{-2}$ . Also plotted is the linear relationship for normal ellipticals from Paper II. It is notable that the envelopes follow an extension to the same structural relation as ellipticals. In terms of structure, the only differences between bright ellipticals and cD envelopes are their large-scale lengths and extremely low effective surface brightnesses. Values of  $\mu_e$  less than  $29V$  mag arcsec $^{-2}$  are artifacts of very shallow envelope slopes and do not reflect real values from the surface brightness data. The above discussion is not meant to impose the same physics of galaxy structure to cD envelopes since the inadequacy of the  $r^{1/4}$  relation is well known (see Djorgovski 1985). However, the extension of the relationship in Figure 4 of Paper II to cD envelopes is interesting and warrants further investigation.

The envelope slopes from power law fits,  $\beta$ , are listed in Table 1. When converted to volume density, the value for an average of all the envelopes in this sample would imply a rela-

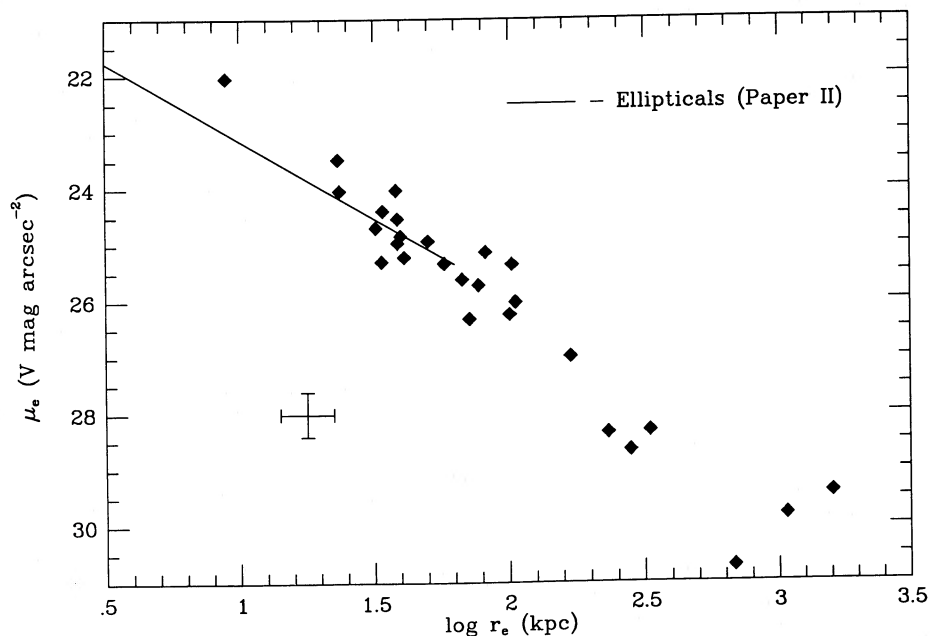


FIG. 4.—Effective surface brightness,  $\mu_e$ , vs. the effective radius,  $r_e$ , for cD envelopes. Characteristic scale lengths for envelopes can range from 10 kpc to 1 Mpc. The solid line is the relationship for normal ellipticals from Paper II. cD envelopes appear in this diagram to be merely larger scaled versions of bright ellipticals.

tion of

$$\rho_{\text{env}} \propto r^{-2.6 \pm 0.3}. \quad (1)$$

For comparison, the distribution of galaxies in cluster density profiles between 100 and 500 kpc (West, Dekel, and Oemler 1987) is given by

$$\rho_{\text{gal}} \propto r^{-2.6 \pm 0.4} \quad (2)$$

in excellent agreement with the envelopes. Another probe of the outer galaxy potential is given by the distribution of globular clusters. Unfortunately, no cD galaxies are sufficiently nearby for globular cluster counts. The best example for comparison is the data of Harris (1986), which studied the distribution of globular clusters around the giant elliptical M87 in Virgo, a galaxy with an "incipient" cD envelope (White 1987). His result gives

$$\rho_{\text{glob}} \propto r^{-2.6} \quad (3)$$

also in agreement with the mean for envelope slopes (for a different value of  $r^{-2.1}$  see Grillmair, Pritchet, and van den Bergh 1986). The *Einstein* X-ray data from (Jones and Forman 1984; Sarazin 1987) was also examined. For the objects in common, a mean density relation of the intracluster gas is

$$\rho_{\text{gas}} \propto r^{-2.1 \pm 0.2}. \quad (4)$$

This is marginally inconsistent with the optical data (see also White and Sarazin 1987) and while cD envelopes follow the distribution of the other luminous material in the cluster potential (i.e., galaxies and globular clusters), they are not distributed in the same fashion as the X-ray-emitting gas.

In order to more fully understand the connection between cD envelopes and the cluster potential, a simple two-component model can be formulated. This model attempts to incorporate our present knowledge of the dynamics of clusters and giant ellipticals as well as the structural information from this data set. The basic assumption for this model is that the kinematics of a cD galaxy can be broken down into an underlying parent galaxy, with attributes similar to a BCM, plus an independent halo component which is more closely associated with the cluster dynamics. Following a method similar to Tonry (1985), a general density distribution of

$$\rho(r) = \rho_0(1 + r^2/r_0^2)^\beta \quad (5)$$

can be adopted for each component where  $\rho_0$  is the central density and  $r_0$  is the core radius. If the motions in each component are isotropic, then hydrostatic equilibrium yields

$$\sigma^2(r) = 4\pi G \rho_0 r_0^2 f(r, \beta), \quad (6)$$

where  $\sigma(r)$  is the one-dimensional velocity dispersion and  $f(r, \beta)$  is a function that can be determined analytically or numerically depending on the value of  $\beta$ . A boundary condition at  $r=0$  will produce an equation which allows the central density to be defined in terms of a central velocity dispersion and core radius. Thus, the variables for each component of this model are  $\sigma_0$ ,  $r_0$ ,  $\beta$  and the  $M/L$  (see below).

For the underlying BCM, a value of  $\beta_g = -3/2$  is adopted, which for large radii will simulate a King model distribution of  $\rho \propto r^{-3}$ . Although BCMs were shown to be more shallower than King models in Paper II, with  $\rho_g \propto r^{-2.7}$ , for this model the small difference will be ignored. The boundary condition yields an analytic solution for the central density of

$$\sigma_g^2 = 4\pi G \rho_g r_g^2 \left( \frac{3}{2} - 2 \ln 2 \right). \quad (7)$$

With values of  $\sigma_g = 375 \text{ km s}^{-1}$  and  $r_g = 2 \text{ kpc}$  (Malumuth and Kirshner 1985), a central density of  $\rho_g = 5.7 M_\odot/\text{pc}^3$  is derived.

In principle, for the halo component, fits can be made to luminosity profile to determine  $\beta_h$  and  $r_h$ . But, in practice, only  $\beta_h$  can be measured accurately, whereas there will be a range of acceptable  $r_h$  values. Alternatively, cluster values for  $r_h$  and  $\sigma_h$  can be used and are discussed below.

The density distribution in equation (5) will project into a mass surface density of

$$\Sigma(r) = \Sigma_0(1 + r^2/r_0^2)^{\beta+1/2}, \quad (8)$$

where

$$\Sigma_0 = \frac{\pi r_0}{(-\beta - 1/2) \Gamma(1/2) \Gamma(-\beta)} \rho_0. \quad (9)$$

Assuming constant  $M/L$  with radius for each component, we can derive surface luminosity as:

$$I(r) = (M/L)^{-1} \Sigma(r). \quad (10)$$

The galaxy and halo components are then summed to produce the final model. The parent galaxy's values of  $\beta_g$ ,  $r_g$ , and  $\sigma_g$  are stated above plus a value of  $[M/L]_g = 10$  is assumed. For the halo component,  $\beta_h$  is measured directly from the surface brightness profiles. The remaining parameters;  $r_h$ ,  $\sigma_h$ , and  $[M/L]_h$ , can be treated as variables. However, for the process of actually fitting envelopes, there are only two free parameters; a core radius and a central intensity. From equations (6) and (10) it is obvious that  $\sigma_h$  and  $[M/L]_h$  are strongly coupled such that  $I_0 \propto \sigma_h^2 [M/L]_h^{-1}$ . Thus, without dynamical information, it is impossible to resolve the contribution of each term. Instead, for the following discussions, we will consider only the term  $\sigma_h^2 [M/L]_h^{-1}$  as one variable and  $r_h$  as the second.

In Figure 5, five models for various  $r_h$ ,  $\log \sigma_h^2 [M/L]_h^{-1}$  are plotted along with the surface brightness profile of A2670-G1 (Oemler 1973). Adopting the cluster parameters from Tonry (1985) of  $\sigma_h = 1000 \text{ km s}^{-1}$ , a  $M/L = 300(\log \sigma_h^2 [M/L]_h^{-1} = 3.5)$ ,  $r_h = 100 \text{ kpc}$  (180 kpc in projection; Dressler 1978), and an outer slope of  $\beta = -1$  produces a model cD envelope which is much brighter than the average envelopes from this data set (see middle left panel of Fig. 5). Some improvement is made if  $\beta = -1.3$ , the mean envelope slope in Table 1 in space density terms (see bottom left panel in Fig. 5). However, the best fits for cD envelopes were found with values between  $\log \sigma_h^2 [M/L]_h^{-1}$  of 3.2–3.5 and  $r_h$  of 30–100 kpc (see top and middle right panels of Fig. 5). The last panel in Figure 5 demonstrates the failure of the model if a cluster  $\sigma_h$  is used in conjunction with  $[M/L]_h$  of the same value as  $[M/L]_g$ .

A more quantitative analysis can be performed using a  $\chi^2$  test on a range of model types. The resulting  $\chi^2$  distribution for A2670 with  $\sigma_h^2 [M/L]_h^{-1}$  and  $r_h$  as free parameters is shown in Figure 6. As can be seen in the contours, there is a large range of acceptable values for  $\sigma_h^2 [M/L]_h^{-1}$  and  $r_h$  which fit the galaxy plus envelope equally well. For this reason, a rigorous fitting program for each envelope in Table 1 was not attempted. Nonetheless, a range of values is distinct in  $\chi^2$  space, and this type of analysis may prove fruitful when dynamical information for cD envelopes becomes more common.

#### d) Cluster Properties

An assumption that is usually extended to cD galaxies is that cluster-sized objects should in some manner be influenced by,



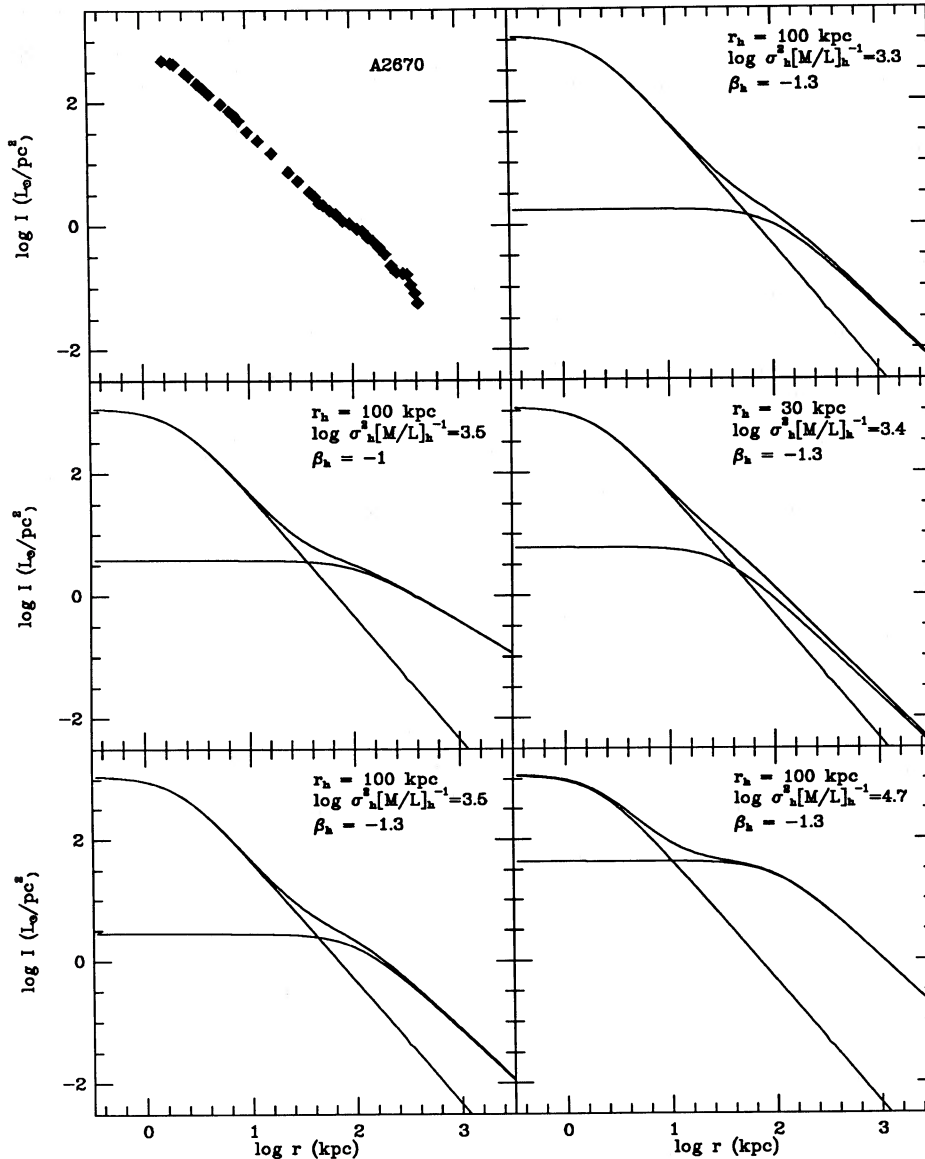


FIG. 5.—Examples of the simple two-component model described in text along with the profile of A2670-G1 (Oemler 1976). Best simulations for all envelopes were found for models with halo velocity dispersions between  $500$  and  $1500 \text{ km s}^{-1}$  and cluster core radii between  $30$  and  $120 \text{ kpc}$ . Adjustments for the envelope  $M/L$  required to match typical envelope luminosities were within the range  $300$ – $500$ .

or have their origin in, the global properties of the cluster (i.e., correlated with richness, velocity dispersion, dynamical state, etc.). In order to test this hypothesis, the envelope luminosities listed in Table 1 are compared to numerous cluster properties found in the literature. In Figure 7,  $\log L_{\text{env}}$  is plotted versus cluster richness as represented by the galaxy counts of Struble and Rood (1987b),  $N_{\text{Abell}}$ . If only compact, regular clusters are considered, then there is a positive correlation ( $R = 0.72$ ) between the number of galaxies in a cluster and cD envelope luminosity of

$$L_{\text{env}} \propto N^{1.62 \pm 0.44} \quad (11)$$

It is plausible that for the irregular clusters (*open symbols* in Fig. 7) their lumpy, distorted appearance reflects an equally complex potential, and that the global richness value of the whole cluster is unrelated to the local environment of the cD envelope. The simple stripping model to form cD envelopes

developed by Malumuth and Richstone (1984) predicts  $L_{\text{env}} \propto N^2$  (also shown in Fig. 7) which is within the errors of equation (11).

Stripping models also predict a correlation with cluster velocity dispersion. No correlation was found between  $L_{\text{env}}$  and the cluster velocity dispersion (not shown); however, the number of clusters in this sample with measured velocity dispersions (Struble and Rood 1987a) is very small and values may be blurred by subcluster effects.

The Bautz-Morgan (BM) type (Bautz and Morgan 1970; Leir and van den Bergh 1977) is assumed to be a coarse indicator of the dynamical state of cluster in terms of dominance of central member and compact nature of inner core region. The relationship between this indicator and  $L_{\text{env}}$  is displayed in Figure 8. The top panel in Figure 8 shows the percentage of occurrences from the original sample of Paper II of cD envelopes versus the BM type of the cluster. The complete

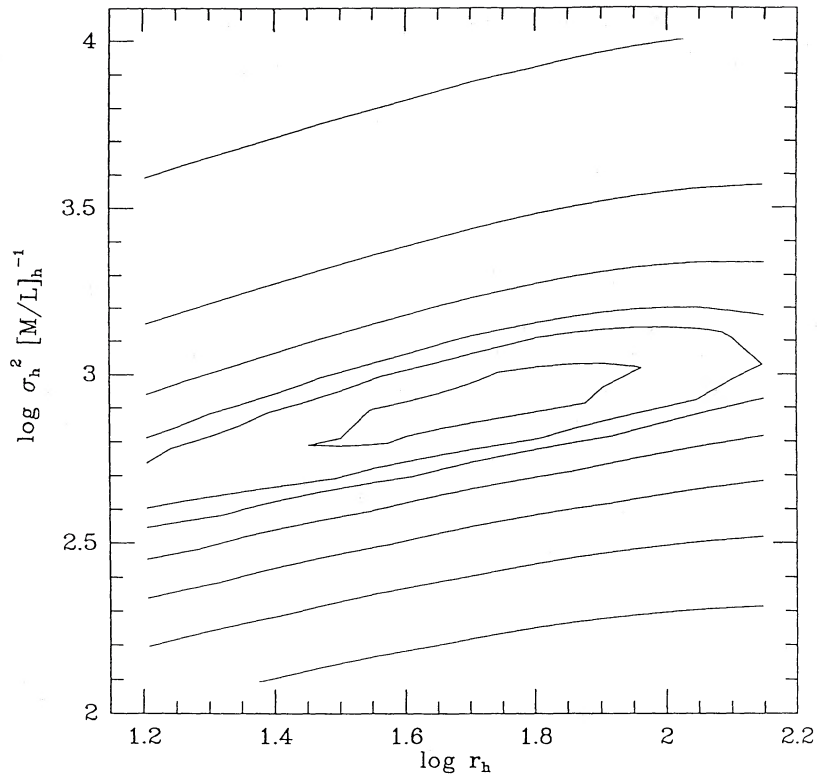


FIG. 6.— $\chi^2$  contours for two-component fits to A2670. Since  $\sigma_h$  and  $[M/L]_h$  are strongly coupled, the two free parameters are  $\sigma_h^2 [M/L]_h^{-1}$  and  $r_h$ . The lowest contour represents a  $\chi^2$  of 1.0 with an increase of 20% for each outer contour. The range of acceptable fits cover halo radii values from 25 to 80 kpc.

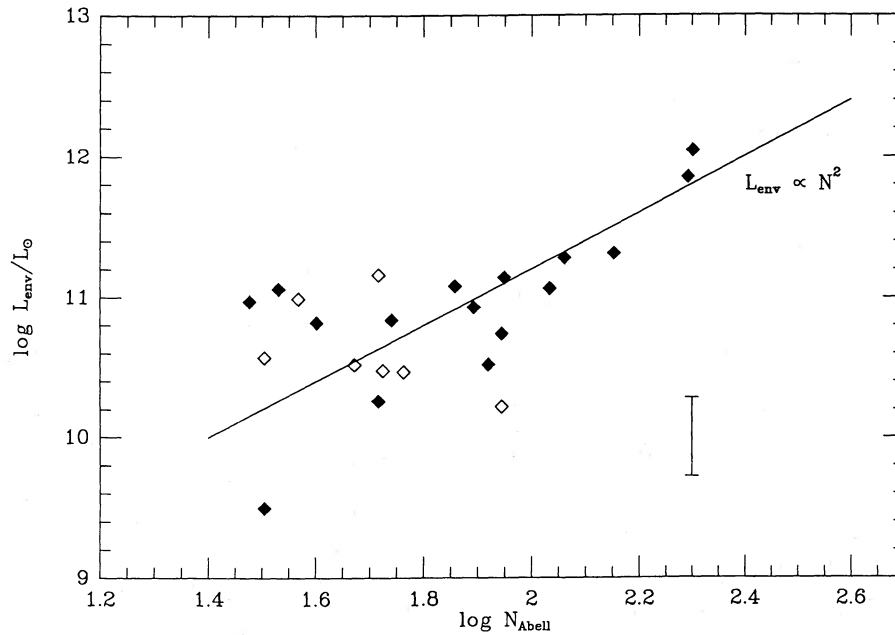


FIG. 7.—Envelope luminosity vs. cluster richness represented by galaxy counts ( $N_{\text{Abell}}$ ; see Struble and Rood 1987b). The predicted relation between envelope luminosity and cluster richness from the stripping models of Malumuth and Richstone (1984) is shown. Solid symbols are for regular, compact clusters (RS types cD, B, and C). Open symbols are for irregular, highly subclustered clusters (RS types F, L, and I).

sample from Paper II (*inset*) was selected to cover a full range of BM types (i.e., a range of cluster environments). Note that over half the BM types I and I-II clusters have cD envelopes, whereas less than one-third of types II through II-III have envelopes. In the bottom panel of Figure 8, the relationship between  $L_{\text{env}}$  and BM type is shown. The scatter is large, but the tendency does exist for envelope luminosity to increase with more highly evolved clusters. The top two ranked envelopes are both in BM type I clusters.

A similar relationship is found between  $L_{\text{env}}$  and Rood-Sastry (RS) type (Struble and Rood 1987*b*), where the RS type is also assumed to be some visual measure of the evolutionary state of a cluster. The top panel in Figure 9 displays the percentage of occurrences from the original sample of Paper II of cD envelopes versus the RS type of the cluster. As in Figure 8, the complete sample from Paper II is shown. Again, half the RS type cD clusters have cD envelopes, whereas less than one-third of all other RS types are found to have envelopes. In the bottom panel of Figure 9 the relationship between  $L_{\text{env}}$  and RS type is plotted. The large scatter makes any correlation indistinct, but the tendency exists for brighter envelopes in more evolved clusters.

The correlation between  $L_{\text{env}}$  and  $L_x$ , found in Figure 10, is the strongest evidence presented linking envelopes to the cluster dynamical state. The X-ray data (Jones and Forman 1985; Valentijn and Bijleveld 1983) fitted by a least-squares algorithm ( $R = 0.84$ ) produces

$$L_{\text{env}} \propto L_x^{1.06 \pm 0.18} \quad (12)$$

The  $L_x$  value for most poor clusters is less than  $10^{42}$  ergs  $\text{s}^{-1}$  (Valentijn and Bijleveld 1983; Bahcall 1980) which from this diagram would predict  $L_{\text{env}}$  of less than  $10^9 L_\odot$ , a value which is not measurable by the techniques used here. The underlying physics in this relation is that a higher X-ray luminosity implies more hot gas and a deeper cluster potential, both resulting from a cluster that has undergone a degree of evolution sufficient to strip gas from spirals and relax the distribution. Therefore, the luminosity of the envelope is somewhat dependent on the local gravitational field of the cluster. This supports the stripping hypothesis since high gradients provide greater probability of tidal interaction. Since the connection between location of first-ranked ellipticals and the X-ray centers of clusters is also strong (Beers and Tonry 1986),  $L_x$  has the advantage of being both a global property of the cluster

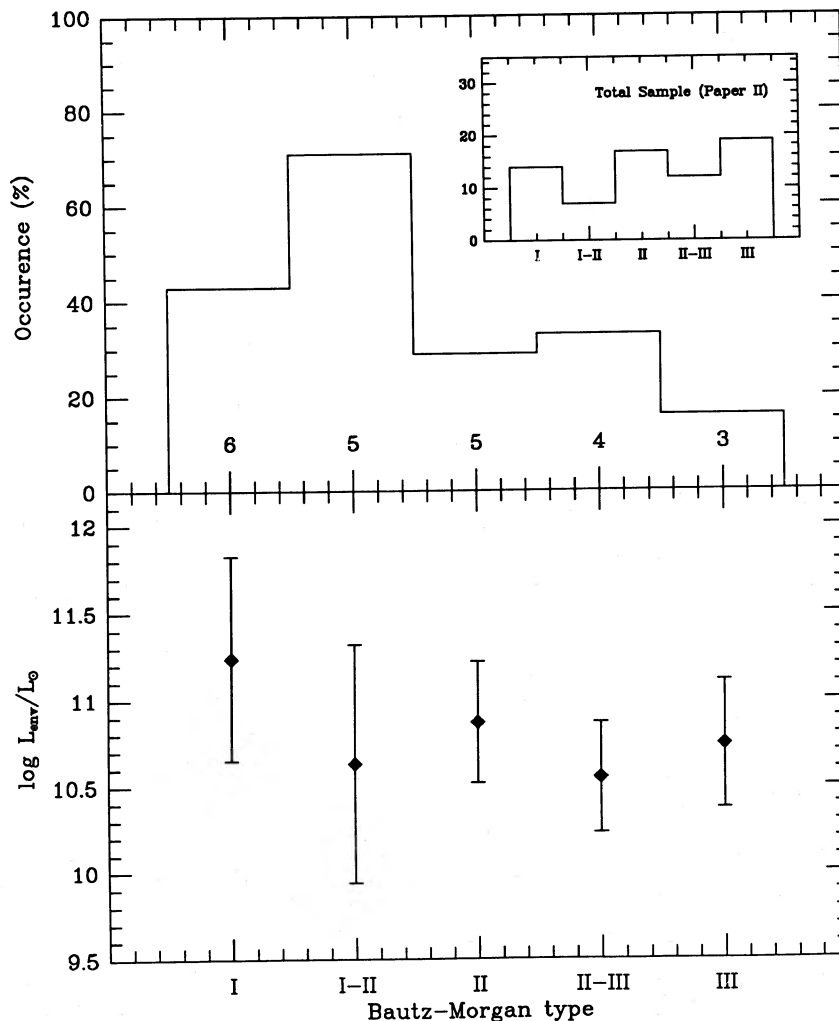


FIG. 8.—Envelope occurrence and luminosities vs. the Bautz-Morgan type of the cluster, a dynamical state indicator. Actual numbers from the complete sample of Paper II (*inset*) are marked. Although most of the envelopes were found in BM type I and I-II clusters, the number found in less evolved clusters is significant. A tendency for envelope luminosity to increase with the more evolved clusters is suggested.

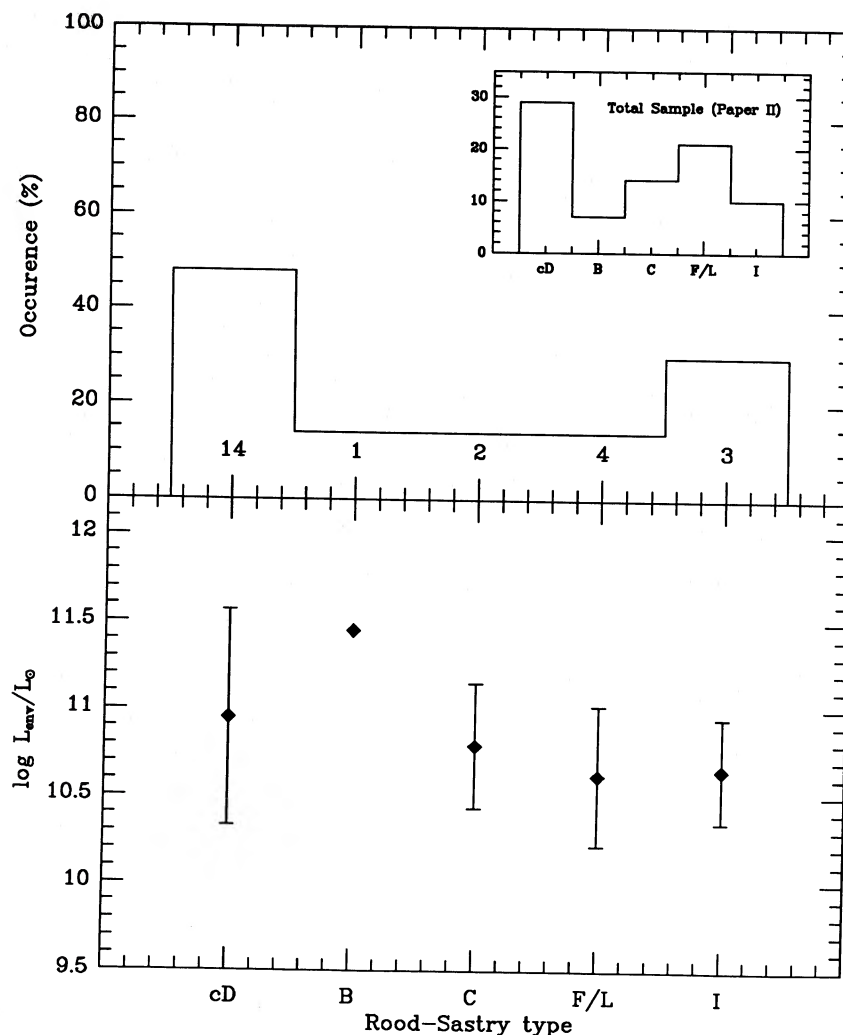


FIG. 9.—Envelope occurrence and luminosities vs. the Rood-Sastry type of the cluster. Actual numbers from the complete sample of Paper II (*inset*) are marked. The greatest occurrence of envelopes are in cD type clusters. The high fraction of envelopes in type I systems may be reflecting the importance of rapid evolution in the small subgroups that dominate in these types of clusters. As in Fig. 7, a tendency for envelope luminosity to increase with the more evolved clusters is suggested.

and a local measure of the potential near the cD galaxy. This may explain the tighter correlation in Figure 10 versus the indistinct correlations in Figures 8 and 9 since Bautz-Morgan and Rood-Sastry type are relatively insensitive to the amount of subclustering.  $L_x$  is also a more direct measure of the evolution of the cluster potential regardless of subclustering.

A significant fraction of cD envelopes were found in irregular clusters (Rood and Sastry types L, F, and I or BM types II through III; see Figs. 8 and 9). To investigate the occurrence of envelopes in the field, 24 galaxies from Paper II were selected from the KOSS redshift survey (Kirshner *et al.* 1983) with the constraints of extreme brightness and isolation from other galaxies. *No envelopes were found in this field sample, and, therefore, a cluster or subcluster environment is a prerequisite for cD envelopes.* The envelopes discussed here were all located in a cluster core or in the center of a local subcluster. No extended envelopes were found in the 12 poor clusters examined with the possible exception of AWM 7, a bright elliptical with peculiar extended structure but unlike a normal cD galaxy. A corollary to this statement is that a minimal cluster richness is required before the envelope luminosity crosses the  $10^9 L_\odot$  threshold to be detected as an independent component.

#### IV. CONCLUSIONS

The observations and interpretation of the various correlations presented in this study can be summarized as the following:

1. cD envelopes are best discovered with photographic material which provides good plate scale for sufficient sky contrast. The field size for most CCD systems are too small without reimaging optics to cover the entire envelope in a single frame. Comparison to elliptical templates allows the determination of an envelope luminosity independent of the underlying galaxy (see Table 1).
2. A correlation between the luminosity of the parent galaxy and the envelope luminosity indicates that similar processes (i.e., dynamic) are responsible for the formation of BCMs and cD envelopes.
3. cD envelopes are found in a range of cluster environments, from regular, compact clusters to irregular, highly subclustered systems. However, there is a higher rate of occurrence and higher luminosity envelopes in the more evolved clusters.
4. cD envelopes can be found around non-first-ranked ellip-

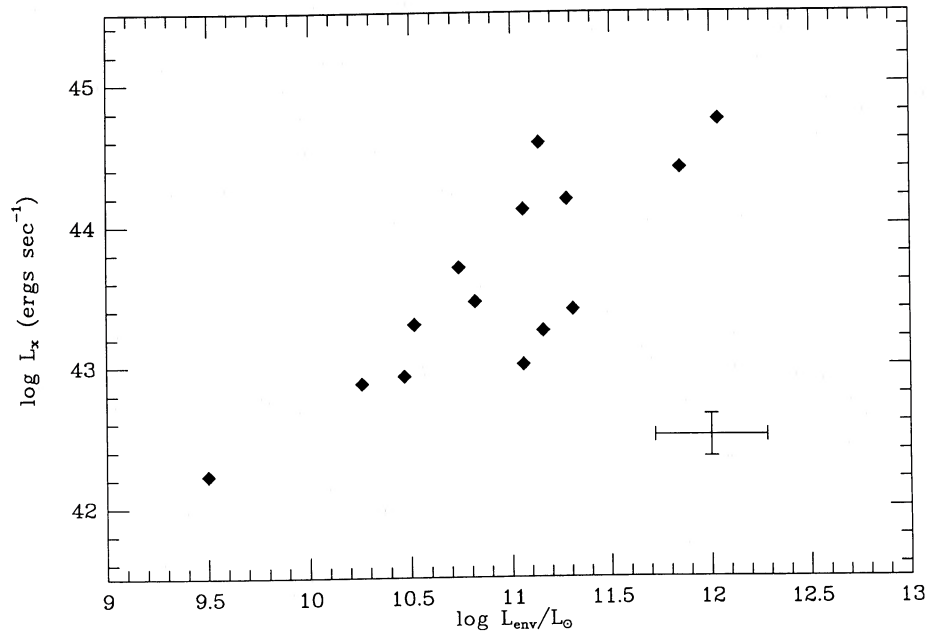


FIG. 10.—Total cluster X-ray luminosity (Valentijn and Bijveld 1983) vs. envelope luminosity. This correlation ( $R = 0.72$ ) is the strongest evidence in this study for a link between the dynamical state of a cluster and the luminosity of the cD envelope.

ticals such as NGC 4839 in Coma (Oemler 1976) and NGC 6034 in Hercules (Schombert 1984). However, all envelopes were found at local cluster density maxima (see also Beers and Geller 1983) and none was discovered in the field.

5. The envelope colors of three cD galaxies display no large deviations from the red color of the parent galaxy. This observation is a direct contradiction with the blue colors in cD envelopes found by Valentijn (1983).

6. The surface brightness profiles of cD envelopes are well fitted by the  $r^{1/4}$  law extending the relationship of characteristic surface brightness and radii for BCMs from Paper II to cluster scale lengths. The power-law slopes of cD envelopes follow the same form as other luminous material in clusters (i.e., galaxies and globular clusters;  $\rho \propto r^{-2.6}$ ), but do not conform to the distribution of hot X-ray gas ( $\rho \propto r^{-2.1}$ ; Jones and Forman 1984).

7. A two-component model, combining an underlying galaxy plus a separate halo component, is constructed. The range of halo velocity dispersion,  $[M/L]$ , and core radius which provide acceptable fits is too large to constrain the true values without dynamical information. Normal cluster parameters (i.e.,  $\sigma_h = 1000 \text{ km s}^{-1}$ ,  $[M/L]_h = 300$ , and  $r_h = 100 \text{ kpc}$ ) are as equally plausible as models with small core radii (30 kpc) and low  $\sigma_h$ . However, for the larger cD envelopes, a distinct inflection point in the surface brightness profile is visible, indicating cluster scale lengths for many bright envelopes.

8. The envelope luminosity is weakly correlated with several global cluster properties. Most importantly for the stripping hypothesis is the confirmation of a correlation between cluster richness and envelope luminosity predicted by the models of Malumuth and Richstone (1984). In the sense that highly evolved clusters are more likely to have brighter cD envelopes, the strength and occurrence of envelopes are also correlated with the dynamical state of the cluster, as estimated from Bautz-Morgan and Rood-Sastry classification. This is also seen in the relationship between cD envelope and the X-ray luminosity of the cluster, which is assumed to be a direct

measure of the depth of the cluster potential, and a strong indicator that cD envelopes are directly linked to the evolution of the cluster potential. Of course, the reverse causality situation must also be considered; cD envelopes induce more rapid cluster evolution and, thus, the envelope itself may be responsible for the high X-ray luminosity and deeper potential.

Although the data present here cannot definitively determine which formation theory for cD envelopes is correct, the observations can discriminate between various predictions and provide more information for speculation. For example, based on the red envelope colors it is clear that recent star formation has not occurred in cD envelopes. In fact, since the colors of the envelopes are so similar to the colors of the parent galaxy, it is unlikely that even the biased star formation proposed by Fabian, Nulsen, and Canizares (1984) for cooling flows can reproduce the expected mass and  $M/L$  suggested by the two component model. While this process may result in an increased gas density in the inner 10 kpc of the elliptical and the formation of new stars in the centers of cD galaxies (Romanishin 1986), it is implausible as a method to form extended envelopes. Based on energy considerations and comparison to  $N$ -body simulations, mergers can also be eliminated as a source of envelope material.

The correlation between cD envelopes and cluster evolutionary state would argue strongly for a process that is linked to the dynamical state of the cluster, such as stripping. However, the fact that this tidal debris has the same distribution as other cluster material, extends several cluster core radii and has an apparently old stellar population implies that the formation process occurred very early, before cluster collapse and virialization, much in the manner as proposed by Merritt (1984). This would also explain why envelopes are found within local subgroups of irregular clusters.

Most interesting for future work in this area is the idea suggested by the two component model that the halos parameters may reflect actual cluster potential values. Certainly, detailed comparison of cD envelope contour maps with X-ray

contours and galaxy counts will yield information on the shape of cluster potentials. Future work in progress to determine the stellar populations, velocity dispersions, and the orbits of galaxies within cD envelopes will also help resolve many of questions left unanswered by this paper.

The author wishes to thank J. Tonry for in-depth discussions and excellent refereeing, particularly with respect to the two-

component model. The author also wishes to thank G. Bothun for suggesting and developing the double blind method of testing color gradients in envelopes. A special thanks is extended to G. Oemler for supporting this project in its youth. This work has also benefited from many stimulating discussions with D. Merritt, F. Schweizer, and M. West. J. Phinney is thanked for his efficient handling of the Palomar 1.5 m telescope. This project was supported on NSF grant AST84-16704.

## REFERENCES

- Bahcall, N. A. 1980, *Ap. J. (Letters)*, **238**, L117.  
 Baum, W. A., Thomsen, B., and Morgan, B. L. 1986, *Ap. J.*, **301**, 83.  
 Bautz, L. P., and Morgan, W. W. 1970, *Ap. J. (Letters)*, **162**, L149.  
 Beers, T. C., and Geller, M. J. 1983, *Ap. J.*, **274**, 491.  
 Beers, T. C., and Tonry, J. L. 1986, *Ap. J.*, **300**, 557.  
 Cowie, L. L., and Binney, J. 1977, *Ap. J.*, **215**, 723.  
 Djorgovski, S. 1985, Ph.D. thesis, University of California, Berkeley.  
 Dressler, A. 1978, *Ap. J.*, **226**, 55.  
 ———. 1979, *Ap. J.*, **231**, 659.  
 ———. 1980, *Ap. J.*, **236**, 351.  
 Duncan, M. J., Farouki, R. T., and Shapiro, S. L. 1983, *Ap. J.*, **271**, 22.  
 Fabian, A. C., and Nulsen, P. E. J. 1977, *M.N.R.A.S.*, **180**, 479.  
 Fabian, A. C., Nulsen, P. E. J., and Canizares, C. R. 1984, *M.N.R.A.S.*, **201**, 933.  
 Fitchett, M., and Webster, R. 1987, *Ap. J.*, **317**, 653.  
 Gallagher, J. S., and Ostriker, J. P. 1972, *A.J.*, **77**, 288.  
 Grillmair, C., Pritchet, C., and van den Bergh, S. 1986, *A.J.*, **91**, 1328.  
 Harris, W. 1986, *A.J.*, **91**, 822.  
 Jones, C., and Forman, W. 1984, *Ap. J.*, **276**, 38.  
 Kirshner, R. P., Oemler, A., Schechter, P. L., and Shectman, S. A. 1983, *A.J.*, **88**, 1285.  
 Lauer, T. R. 1987, preprint.  
 Leir, A. A., and van den Bergh, S. 1977, *Ap. J. Suppl.*, **34**, 381.  
 Lugger, P. M. 1984, *Ap. J.*, **278**, 51.  
 Malumuth, E. M. 1983, Ph.D. thesis, University of Michigan.  
 Malumuth, E. M., and Kirshner, R. P. 1981, *Ap. J.*, **251**, 508.  
 ———. 1985, *Ap. J.*, **291**, 8.  
 Malumuth, E. M., and Richstone, D. O. 1984, *Ap. J.*, **276**, 413.  
 Matthews, T. A., Morgan, W. W., and Schmidt, M. 1964, *Ap. J.*, **140**, 35.  
 Merritt, D. 1984, *Ap. J.*, **276**, 26.  
 Oemler, A. 1973, *Ap. J.*, **180**, 11.  
 ———. 1976, *Ap. J.*, **209**, 693.  
 Porter, A. 1987, Ph.D. thesis, California Institute of Technology.  
 Richstone, D. O. 1976, *Ap. J.*, **204**, 642.  
 Romanishin, W. 1986, *Ap. J.*, **301**, 675.  
 Sarazin, C. L. 1987, in Proc. of the Greenbank Workshop on Continuum Radio Processes in Clusters of Galaxies, in press.  
 Sandage, A. R., and Hardy, E. 1973, *Ap. J.*, **183**, 743.  
 Schneider, D. P., and Gunn, J. E. 1982, *Ap. J.*, **263**, 14.  
 Schneider, D. P., Gunn, J. E., and Hoessel, J. G. 1983, *Ap. J.*, **268**, 476.  
 Schombert, J. M. 1984, Ph.D. thesis, Yale University.  
 ———. 1986, *Ap. J. Suppl.*, **60**, 603 (Paper I).  
 ———. 1987, *Ap. J. Suppl.*, **64**, 643 (Paper II).  
 ———. 1988, in preparation.  
 Schombert, J. M., and Bothun, G. D. 1987, *A.J.*, **92**, 60.  
 Schombert, J. M., and Wallin, J. F. 1987, *A.J.*, **94**, 300.  
 Strom, K. M., and Strom, S. E. 1977, in *The Evolution of Galaxies and Stellar Populations*, ed. B. Tinsley and R. Larson (New Haven: Yale University Press), p. 239.  
 Struble, M. F., and Rood, H. J. 1987a, *Ap. J. Suppl.*, **63**, 543.  
 ———. 1987b, *Ap. J. Suppl.*, **63**, 555.  
 Tonry, J. L. 1985, *Ap. J.*, **291**, 45.  
 ———. 1987, in *IAU Symposium 127, Structure and Dynamics of Elliptical Galaxies*, ed. T. de Zeeuw (Dordrecht: Reidel), p. 89.  
 Valentijn, E. A. 1983, *Astr. Ap.*, **118**, 123.  
 Valentijn, E. A., and Bijleveld, W. 1983, *Astr. Ap.*, **125**, 223.  
 Villumsen, J. V. 1982, Ph.D. thesis, Yale University.  
 West, M. J., Dekel, A., and Oemler, A. 1987, *Ap. J.*, **316**, 1.  
 White, R. E. 1987, *M.N.R.A.S.*, **227**, 185.  
 White, R. E., and Sarazin, C. L. 1987, *Ap. J.*, **318**, 612.  
 White, S. D. M. 1982, in *Saas-Fee Lectures*, ed. L. Martinet and M. Mayer (Geneva: Geneva Observatory), p. 291.

JAMES M. SCHOMBERT: Palomar Observatory, California Institute of Technology, Mail Code 105-24, Pasadena, CA 91125